

## Research Paper

**Cite this article:** Guo F, Castillo P, Li C, Qing X, Li H (2022). Description of *Rotylenchus zhongshanensis* sp. nov. (Tylenchomorpha: Hoplolaimidae) and discovery of its endosymbiont *Cardinium*. *Journal of Helminthology* **96**, e48, 1–13. <https://doi.org/10.1017/S0022149X22000384>

Received: 20 April 2022  
Accepted: 13 June 2022


**Key Words:**

Bacterial cyto-endosymbiont; genome assembly; molecular; morphology; new species; phylogeny; plant-parasitic nematode; taxonomy

**Author for correspondence:**

Xue Qing,  
E-mail: [qingxue@njau.edu.cn](mailto:qingxue@njau.edu.cn)

# Description of *Rotylenchus zhongshanensis* sp. nov. (Tylenchomorpha: Hoplolaimidae) and discovery of its endosymbiont *Cardinium*

F. Guo<sup>1,2</sup>, P. Castillo<sup>3</sup>, C. Li<sup>1</sup>, X. Qing<sup>1,2</sup>  and H. Li<sup>1,2</sup>

<sup>1</sup>Department of Plant Pathology, Nanjing Agricultural University, Nanjing 210095, People's Republic of China; <sup>2</sup>Key Laboratory of Integrated Management of Crop Diseases and Pests, Ministry of Education, Nanjing Agricultural University, Nanjing 210095, People's Republic of China and <sup>3</sup>Spanish National Research Council (CSIC), Institute for Sustainable Agriculture (IAS), Campus de Excelencia Internacional Agrolimentario, ceiA3, Avenida Menendez Pidal s/n, 14004 Cordoba, Spain

**Abstract**

A new bisexual species of *Rotylenchus* is described and illustrated based on morphological, morphometric and molecular characterizations. *Rotylenchus zhongshanensis* sp. nov. is characterized by having a conoid lip region complying with the basic pattern for Hoplolaimidae, but with pharyngeal glands slightly overlapping intestine dorsally and cuticle thickened abnormally in female tail terminus. Females have robust stylet (30.1–33.8 µm). The pharyngeal gland has short dorsal (11.2–16.8 µm) overlap on the intestine. The vulva is located at 48.0–56.5% of body length, and phasmids are pore-like, 4–6 annuli posterior to the anus. For males, phasmids are pore-like, 11–17 annuli posterior to cloaca. The spicules are ventrally arcuate (21.0–28.5 µm) with gubernaculum in 5–8 µm length. The rRNA and mitochondrial *COI* genes were successfully sequenced from the assembled whole-genome sequences of the new species, and were used for reconstructing the phylogenetic relationships of the new species. A new strain of cyto-endosymbiont *Cardinium* was also discovered from the genome sequences of *R. zhongshanensis* sp. nov. The 16S rRNA phylogeny analyses revealed that this new bacterial strain is closed to that from cyst and root-lesion nematodes.

**Introduction**

Nematodes of the genus *Rotylenchus* Filipjev, 1936 are obligate and migratory ectoparasites of various wild and cultivated plants. They use moderate to strong stylets to penetrate surface root tissues and cause cell necrosis. *Rotylenchus* spp. are widely distributed all over the world and have been recorded from all continents with 103 valid species to date (Castillo & Vovlas, 2005; Vovlas *et al.*, 2008; Atighi *et al.*, 2011, 2014; Cantalapiedra-Navarrete *et al.*, 2012, 2013; Aliramaji *et al.*, 2015; Noruzi *et al.*, 2015; Talezari *et al.*, 2015; Golhasan *et al.*, 2016; Nguyen *et al.*, 2019; Singh *et al.*, 2021). This large number of species complicates the identification process, where polytomous keys comprise a useful and practical tool for species identification (Castillo & Vovlas, 2005). In any case, since several cryptic species have been identified within *Rotylenchus*, integrative taxonomy is essential for species identification (Cantalapiedra-Navarrete *et al.*, 2013; Palomares-Rius *et al.*, 2014; Singh *et al.*, 2021). For these reasons, the development of molecular methods using different fragments of nuclear ribosomal and mitochondrial DNA gene sequences have to be used in DNA barcoding during the last years, leading to an accurate species diagnosis, clarifying phylogenetic relationships and species delimitation under the genus *Rotylenchus* (Vovlas *et al.*, 2008; Atighi *et al.*, 2011, 2014; Cantalapiedra-Navarrete *et al.*, 2012, 2013; Aliramaji *et al.*, 2015; Noruzi *et al.*, 2015; Talezari *et al.*, 2015; Golhasan *et al.*, 2016; Tzortzakakis *et al.*, 2016; Nguyen *et al.*, 2019; Singh *et al.*, 2021).

The bacterial genus *Cardinium* Zchori-Fein *et al.*, 2004 comprises cyto-endosymbionts that are widely present in approximately 7–9% of arthropods (Weeks *et al.*, 2003; Zchori-Fein *et al.*, 2004). The genus *Cardinium* gained major interest as they have evolved to modify their host reproduction through at least three reproductive manipulations, *viz.*, parthenogenesis, feminization and cytoplasmic incompatibility. In phylum Nematoda, *Cardinium* has been recovered primarily from the root-lesion nematode *Pratylenchus penetrans* (Cobb, 1917) Filipjev & Stekhoven, 1941 (Denver *et al.*, 2016; Brown *et al.*, 2018) and *Heterodera avenae* Wollenweber, 1924 in transcriptome analysis (Yang *et al.*, 2017) and also from *Heterodera glycines* Ichinohe, 1952 (Endo, 1979; Noel & Atibalentja, 2006; Showmaker *et al.*, 2018).

In the present study, two populations of the genus *Rotylenchus* were isolated, and subsequently characterized based on molecular and morphological analyses. Through Illumina genome sequencing we also reported the presence of *Cardinium* in the newly described species and its phylogeny was discussed.

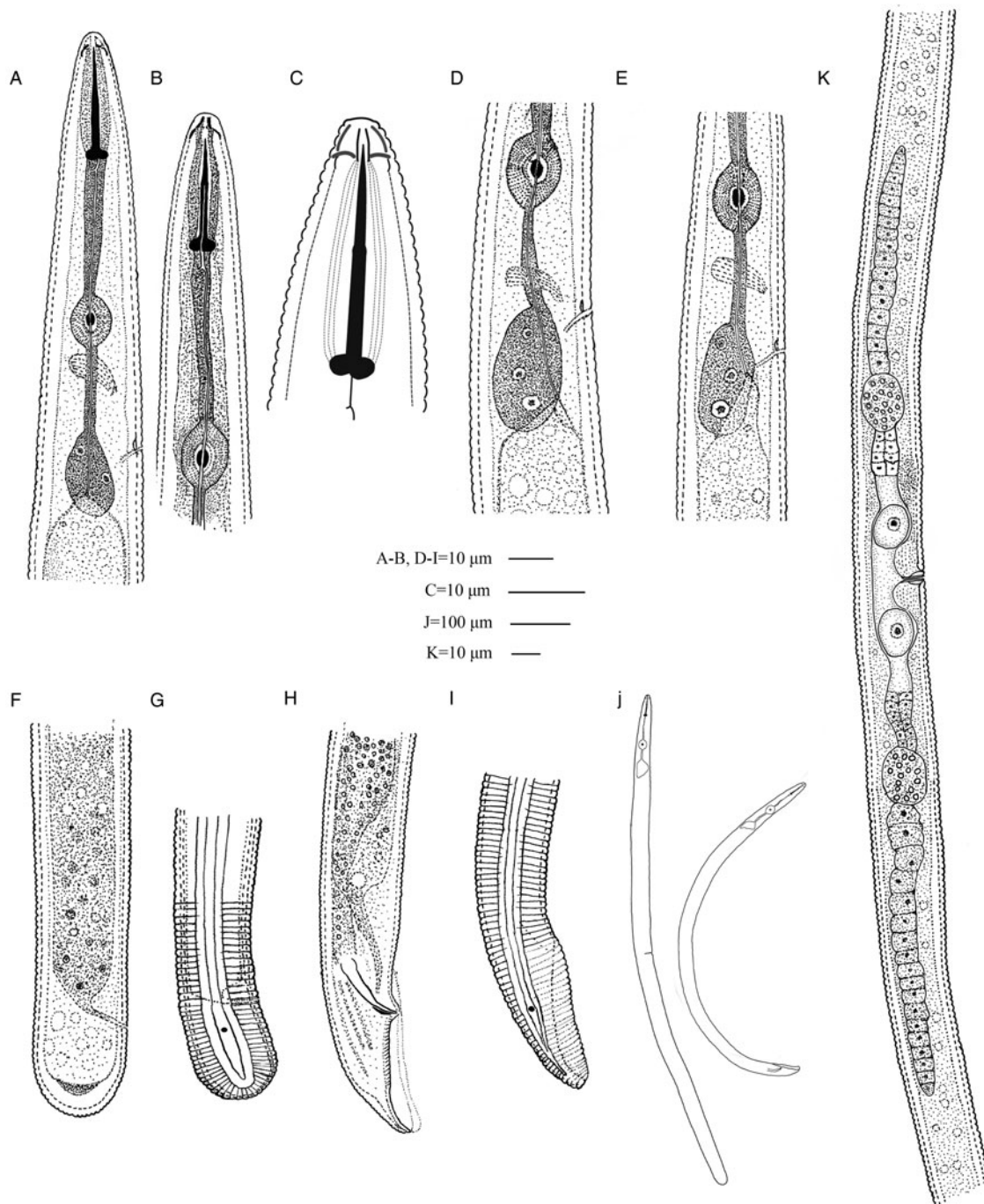


**Fig. 1.** Line drawing of *Rotylenchus zhongshanensis* sp. nov. (NAU population). (a–c): female anterior body region; (d, e): gland overlap; (f, g): female tail region; (h, i): male tail region; (j): female (left) and male (right) body outline; (k): female reproductive system.

## Materials and methods

### *Nematode sampling and morphological analyses*

The nematodes were extracted from soil using a modified Baermann tray method (Whitehead & Hemming, 1965). The extracted fresh nematodes were fixed in 4% formalin solution at 60°C, and gradually transferred to anhydrous glycerin for permanent slides (Sohlenius & Sandor, 1987). Specimens were examined, photographed and measured by an Olympus BX51 microscope equipped with an Olympus DP72 camera (Olympus Corporation, Tokyo, Japan).

### *DNA extraction and genome sequencing*

About 2000 individual nematodes were manually picked up and morphologically examined before processing for DNA extraction. The extraction started with three repeats of freeze–thaw to break the cuticle, followed by DNA isolation using the Ezup Column Animal Genomic DNA Purification Kit (Sangon Biotech, Shanghai, China). The quantity and quality of acquired DNA were checked using the Qubit® 1× dsDNA HS Detect Kit (Yeasen Biotech, Shanghai, China) on the Qubit® 3.0 Fluorometer. The genomic library preparation was performed

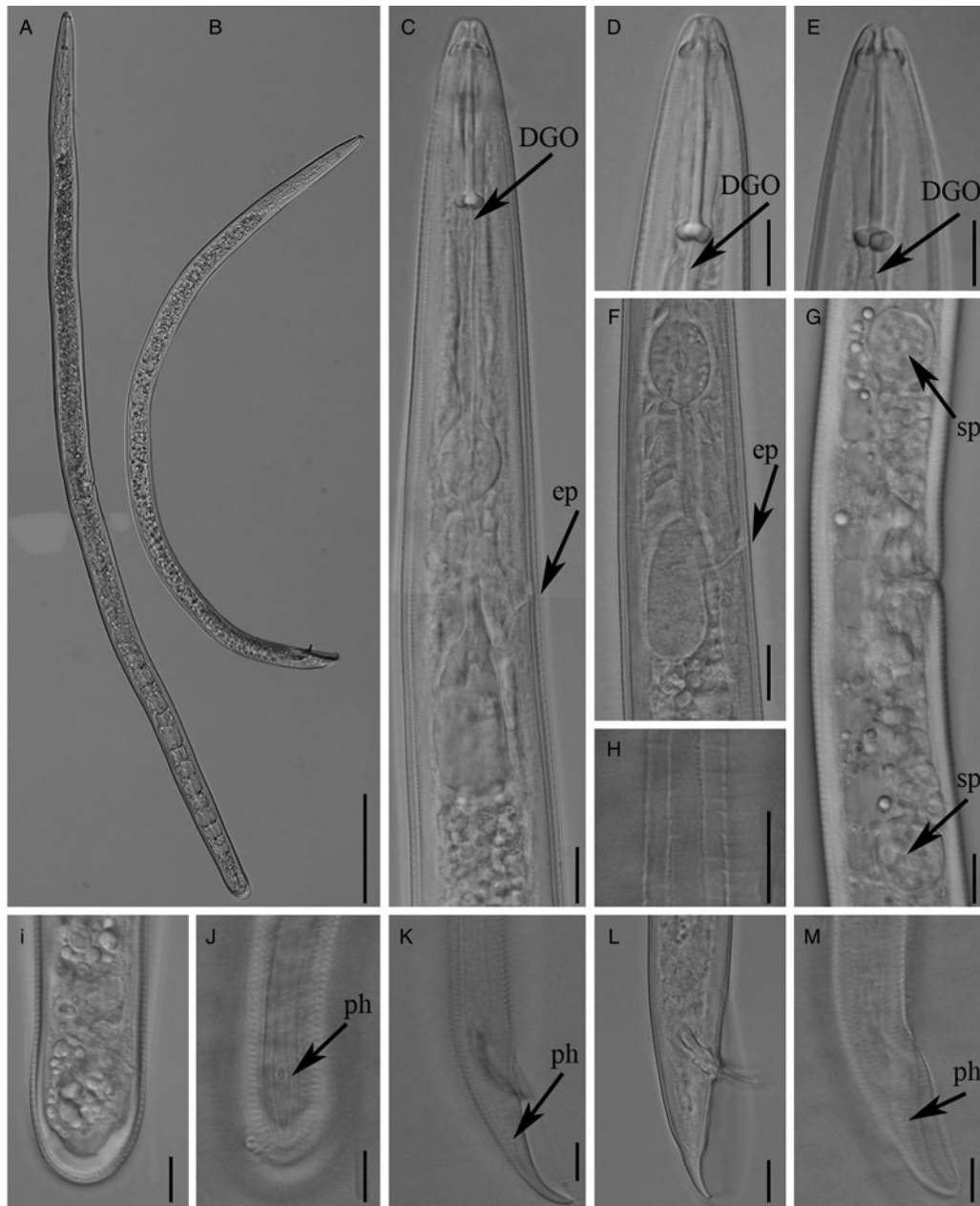


**Fig. 2.** Light micrographs of *Rotylenchus zhongshanensis* sp. nov. (NAU population). (a): female body habitus; (b): male body habitus; (c): pharynx; (d, e): female body anterior end; (f): glands; (g): vulva region; (h): lateral field; (i, j): female tail region; (k–m): male tail region (scale bars: a, b = 100  $\mu$ m; c–m = 10  $\mu$ m). Abbreviations: DGO = dorsal gland orifice; ep = excretory pore; ph = phasmid; sp = spermatheca.

using the Illumina TruSeq DNA Sample Preparation Kit (Personalbio, Shanghai, China). The Illumina Nova Seq 2  $\times$  150 base pairs (bp) paired-end sequencing was performed at Personalgene Corporation (Personalbio, Shanghai, China).

#### Assembly and extraction of nematode barcoding genes

The obtained raw reads from sequencing were first filtered by FastQC (<https://www.bioinformatics.babraham.ac.uk/projects/fastqc/>), then high-quality reads were aligned with the nematode rRNA and mitochondrial genome using the NextGenMap (Sedlazeck *et al.*, 2013). The aligned reads were extracted by SAMtools (Li *et al.*, 2009), subsequently assembled in Novoplasty (Dierckxsens *et al.*, 2017).

The resulting contigs were mapped to available National Center for Biotechnology Information (NCBI) references (rRNA: MZ327998, MZ328000–MZ328003 and Mitogenome: MZ333433, MZ333435–MZ333439) to locate internal transcribed spacer (ITS), 18S rRNA, 28S rRNA and mitochondrial *COI* sequences by using Geneious 7.13.

To validate the Illumina assembled genes and to acquire additional sequences, the traditional polymerase chain reaction (PCR) and Sanger sequencing pipeline was also applied. The 18S rRNA was amplified with primer pairs G18S4 and 18P (Blaxter *et al.*, 1998). The D2–D3 region of 28S rRNA was amplified with newly designed forward primers XQ-D2F (5'- TGG AAA CGG AYA GAG CYA GC-3'), XQ-D2R (5'- GTG TTT CAA GAC

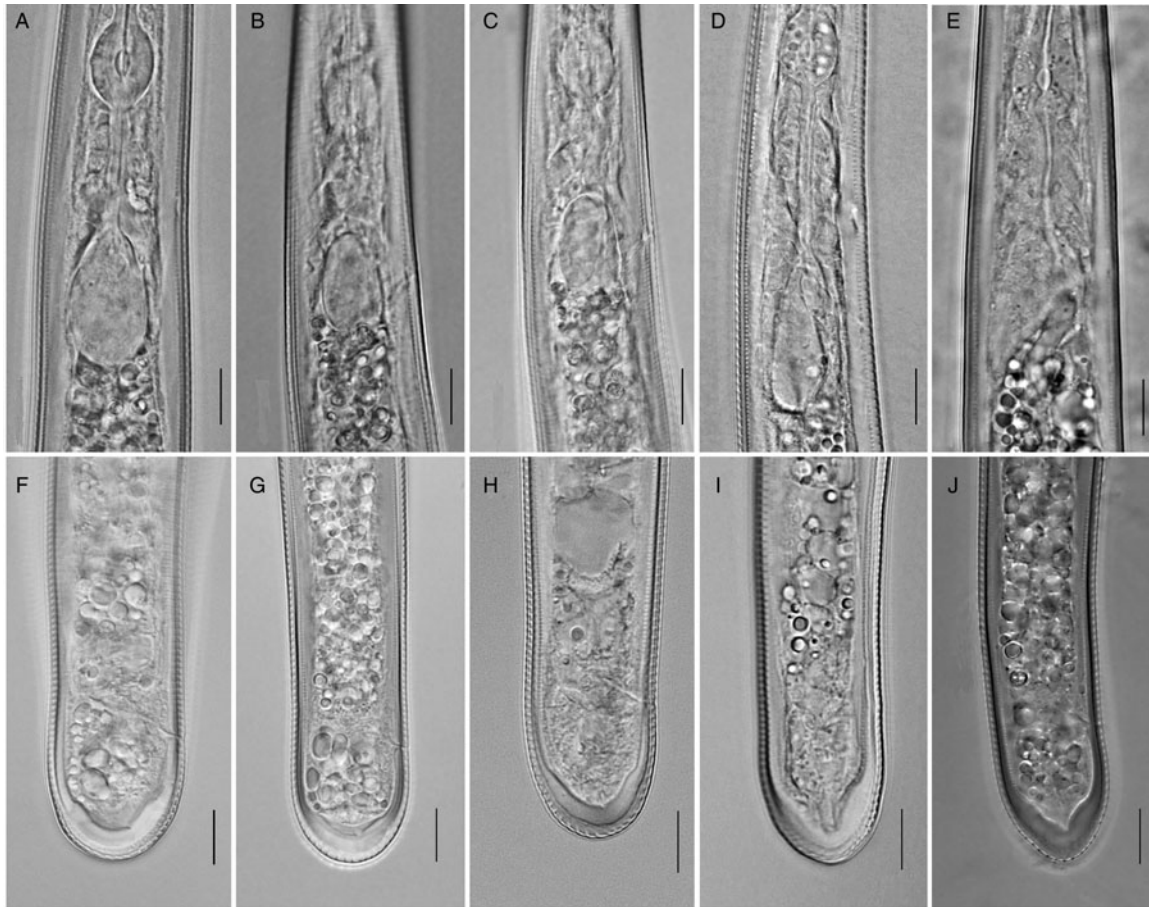


**Fig. 3.** Light micrographs of *Rotylenchus zhongshanensis* sp. nov. (NAU population). (a–e): pharyngeal region of different individuals showing the variations of dorsal pharyngeal overlapping; (f–j): female tail regions in different individuals (scale bars = 10  $\mu$ m).

GGG TCG GA-3'), XQ-D3F (5'- TCC GAC CCG TCT TGA AAC AC-3') and universal reverse primer D3B (Nadler *et al.*, 1999). Briefly, the DNA from a single individual nematode was extracted using worm lysis buffer (Singh *et al.*, 2018) and used as the template. The PCR reaction was carried out in a total volume of 25  $\mu$ l (7.5  $\mu$ l double-distilled water, 2  $\times$  2  $\mu$ l for primers, 12.5  $\mu$ l of Ex Taq DNA polymerase mix and 1  $\mu$ l of DNA template). The thermal cycle program was as follows: an initial step of 95°C for 4 min; 35 cycles of 95°C for 30 s; 54°C for 30 s; 72°C for 2 min; and finished at 72°C for 10 min. The amplified products were purified and subsequently sent for sequencing by Sangon Corporation (Sangon Biotech, Shanghai, China).

### Phylogenetic analyses

The sequences of the new species were compared with those of related species available in GenBank using the Basic Local Alignment Search Tool homology search program. Since the genus *Rotylenchus* is well defined within the family Hoplolaimidae, only species of this taxa were included in the analysis (Nguyen *et al.*, 2019; Singh *et al.*, 2021). Multiple alignments for rRNA genes were built using the G-INS-i algorithm of Multiple Alignment using Fast Fourier Transform v. 7.205 (Kato & Standley, 2013), and the *COI* gene was aligned using TranslatorX (Abascal *et al.*, 2010) under the invertebrate mitochondrial genetic code. To infer phylogenetic trees, Bayesian

inference (BI) and maximum likelihood (ML) analyses were performed on the CIPRES Science Gateway (Miller *et al.*, 2010) using MrBayes 3.2.7 (Ronquist *et al.*, 2012) and RAxML8.1.12 (Stamatakis *et al.*, 2008), respectively. For BI analysis, the GTR +I+G model was selected. The Markov chains were set with four independent chains for  $10 \times 10^6$  generations, sampled every 100 generations, and 25% of the converged runs were discarded as burn-in. For ML analysis, 1000 bootstraps (BS) replicates were included under the GTRCAT model.

### Amplification of 16S rRNA in endosymbiont *Cardinium*

In the process of assembling the *R. zhongshanensis* sp. nov. genome, we found a short sequence belonging to the 16S rRNA gene of a new strain of endosymbiont *Cardinium*. To obtain the full length of the 16S rRNA gene, PCR amplifications were conducted with the DNA template extracted from 2000 individual nematodes mentioned above using two primer pairs. The forward primer 8F (Vandekerckhove *et al.*, 2000) and a newly designed reverse primer CARR1 (5'- TTT TAC GGC CAC TGT CTT CAA GCT CT-3') were used to amplify the 655 bp anterior part of 16S rRNA. The posterior 758 bp was amplified by newly designed forward primer CARF1 (5'- CAG CGG GAC ACT TCG GTG TTG YC-3') and the universal reverse primer 1541R (Vandekerckhove *et al.*, 2000). The obtained *Cardinium* 16S rRNA gene sequences were submitted into the GenBank, and

**Table 1.** Morphometrics of *Rotylenchus zhongshanensis* sp. nov. All measurements are in  $\mu\text{m}$  and in the form: mean  $\pm$  standard deviation (range).

Character	Female		Male
	Holotype	Paratypes	Paratypes
n	1	19	12
L	747.5	789.2 $\pm$ 68.5 (670.0–927.4)	751.3 $\pm$ 29.4 (701.1–807.3)
a	26.5	27.8 $\pm$ 2.3 (22.6–32.2)	31.0 $\pm$ 2.2 (26.5–34.1)
b	6.5	7.0 $\pm$ 0.8 (6.1–9.0)	6.5 $\pm$ 0.4 (6.0–7.5)
b'	5.7	6.3 $\pm$ 0.7 (5.5–8.0)	5.9 $\pm$ 0.4 (5.5–7.0)
C	33.4	31.8 $\pm$ 3.8 (26.5–42.5)	23.7 $\pm$ 2.4 (21.0–28.5)
c'	1.1	1.3 $\pm$ 0.2 (1.0–1.8)	2.1 $\pm$ 0.2 (2.0–2.6)
V/T	54.5	52.7 $\pm$ 1.7 (48.0–56.5)	38.9 $\pm$ 3.8 (32.2–45.2)
stylet	31.4	31.5 $\pm$ 0.8 (30.1–33.8)	29.3 $\pm$ 1.4 (26.8–32.1)
cones	15.3	15.4 $\pm$ 0.6 (14.5–16.8)	14.2 $\pm$ 0.6 (13.2–15.1)
dorsal pharyngeal gland orifice from base of stylet	4.6	4.2 $\pm$ 0.3 (3.7–5.0)	4.5 $\pm$ 0.5 (3.5–5.5)
anterior end to centre of median bulb	73.6	72.0 $\pm$ 3.4 (65.8–80.0)	73.2 $\pm$ 4.7 (66.5–83.0)
anterior end to excretory pore	105.3	103.7 $\pm$ 5.4 (91.3–113.5)	101.1 $\pm$ 3.7 (94.5–109.1)
pharynx length	130.5	126.3 $\pm$ 7.1 (114.6–138.1)	128.0 $\pm$ 8.3 (111.0–141.7)
pharyngeal gland overlapping length	15.4	13.8 $\pm$ 1.2 (11.2–16.8)	11.6 $\pm$ 1.9 (8.5–15.0)
maximum body diameter	28.2	28.6 $\pm$ 3.4 (22.5–34.5)	24.4 $\pm$ 2.1 (22.0–28.8)
anal body diameter	20.2	19.9 $\pm$ 2.3 (15.8–24.0)	15.1 $\pm$ 1.8 (10.1–17.0)
tail length	22.4	25.1 $\pm$ 3.7 (18.5–30.0)	32.0 $\pm$ 2.7 (26.1–35.6)
tail annuli	20	22.8 $\pm$ 2.4 (20–28)	33.7 $\pm$ 3.1 (28–38)
spicule length	–	–	25.7 $\pm$ 1.9 (21.0–28.5)
gubernaculum length	–	–	6.5 $\pm$ 0.7 (5.5–8.0)

compared with those from different host species downloaded from GenBank. The phylogenetic relationship was analysed in the same pipeline of nematode barcoding genes.

## Results

*Rotylenchus zhongshanensis* sp. nov. (The specific epithet refers to Zhongshan Mountain at Nanjing, China, the region from where the new species was recovered.)

*Description* (Nanjing Agricultural University (NAU) type population)

(figs 1–3, table 1)

*Female.* Body cylindrical and relatively small, slightly ventrally curved upon fixation. Lateral field with four smooth equidistant lines, slightly areolated across body. Lip region  $6.8 \pm 0.4$  (6.3–7.7)  $\mu\text{m}$  broad,  $4.7 \pm 0.4$  (4.1–5.8)  $\mu\text{m}$  high, conoid, truncate and continuous, with four or five annuli, framework sclerotization strong, outer margin extending for 2–3 annuli posteriorly into the body. Stylet robust with rounded basal knobs, conus occupying 47.2–51.8% of total length. Dorsal pharyngeal gland orifice (DGO) located at 3.7–5.0  $\mu\text{m}$  from stylet base. Procorpus of pharynx cylindrical, median bulb well developed, broadly ovate. Isthmus slender, encircled by nerve ring at mid-point. Excretory pore usually posterior to the level of nerve ring and anterior to pharyngo-intestinal junction. Hemizonid distinct, 2–3 body annuli long, just anterior to excretory pore. Pharyngeal glands elongate to sacciform with

three nuclei (two anterior smaller nuclei and one bigger posterior), overlapping intestine dorsally for 11.2–16.8  $\mu\text{m}$ . Reproductive system didelphic–amphidelphic, genital branches equally developed, at right side of intestine, outstretched ovaries with a single row of oocytes; spermatheca mostly rounded or oval, axial,  $13.2 \pm 1.4$  (12–16.8)  $\mu\text{m}$  long,  $12.7 \pm 1.1$  (10.3–14.4)  $\mu\text{m}$  wide. Sperm spherical with nucleus occupies the whole cell volume. Vulva 48.0–56.5% of body length from anterior end. Epiptygmata and vulva flap indistinct. Phasmids pore-like, 4–6 annuli posterior to level of anus. Tail short, hemispherical, with 20–28 annuli, terminus cuticle intensified.

*Male.* Less abundant than females. Morphology is similar to females, except for the following characters: body curved ventrally to open C-shaped when heat-killed. Pharyngeal overlapping slightly shorter than that of females. Testis single, anteriorly outstretched, 260–332  $\mu\text{m}$  long. Spicules ventrally arcuate. Gubernaculum protrusible. Phasmid pore-like, 11–17 annuli posterior to cloacal aperture. Tail conoid, 26.1–35.6  $\mu\text{m}$  long or nearly 1.8–2.5 times of cloacal opening diameter. Bursa 39.3–54.5  $\mu\text{m}$  long, completely surrounding tail.

## Type host and locality

Type population of *R. zhongshanensis* sp. nov. was recovered from the rhizosphere soil of several types of grasses including *Digitaria sanguinalis*, *Cynodon dactylon* and *Erigeron acer* located at the

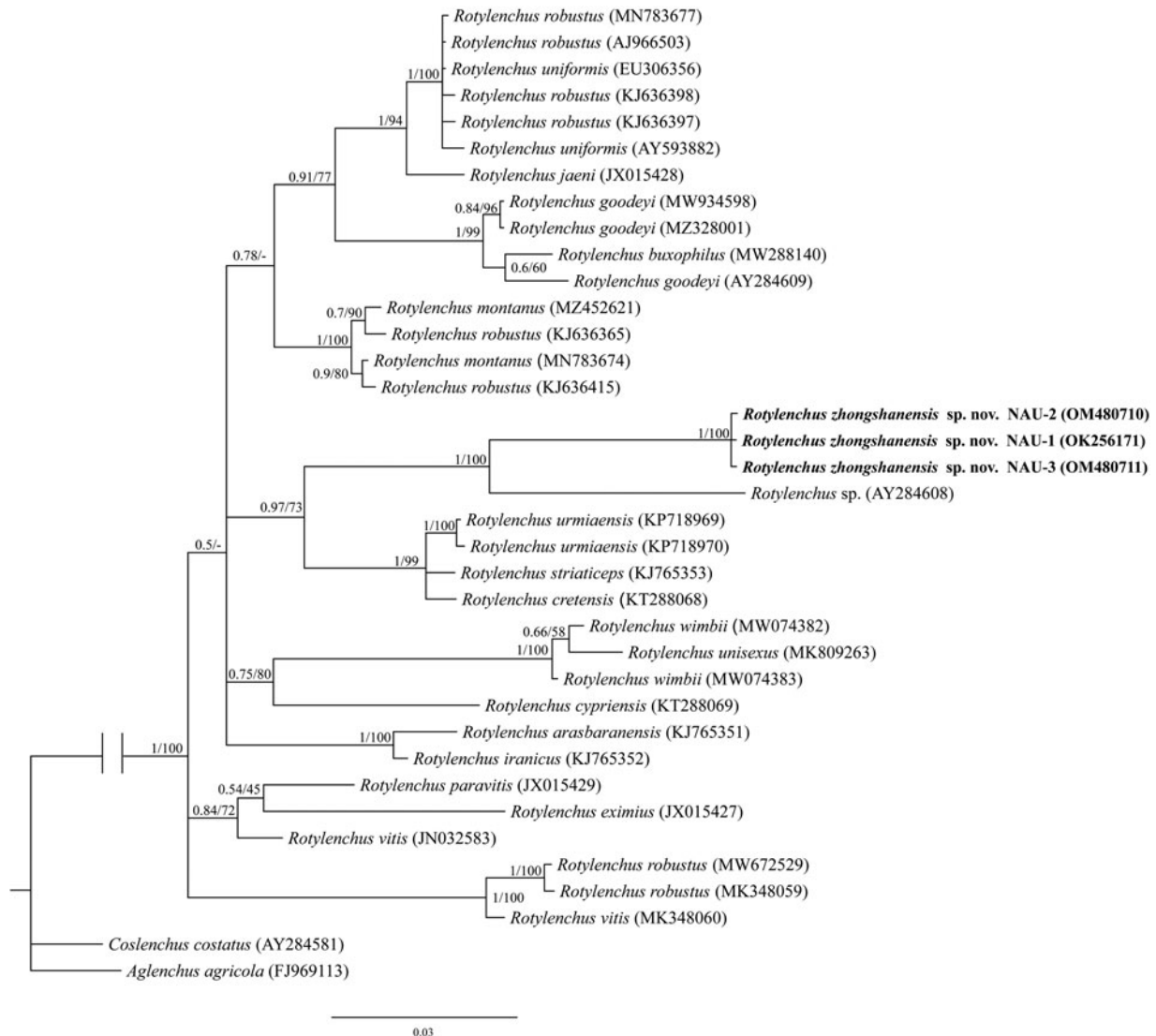


**Fig. 4.** Bayesian 50% majority-rule consensus tree of *Rotylenchus zhongshanensis* sp. nov. and other related nematodes inferred from 18S rRNA gene. Dataset aligned with G-INS-i implemented in Multiple Alignment using Fast Fourier Transform. The values at clade node indicate as posterior probability/bootstrap. Newly obtained sequence is indicated in boldface type. The scale bar indicates expected changes per site.

campus of Nanjing Agricultural University, Nanjing, China (Global Positioning System (GPS) coordinates: 32°02'17"N, 118°51'07"E, NAU population).

#### Other locality

An additional population was found in Zhongshan Mountain of Nanjing, China (GPS coordinates: 32°03'15"N, 118°51'46"E, Zhongshan, ZS) population) in the soil of deciduous forest. This population was only used for molecular study since only a few juveniles were recovered.

#### Type material

Three female paratypes, in one slide, was deposited at the Ghent University Museum, Zoology Collections, collection number UGMD 104438. Holotype female, paratype males and females and juveniles (20 females, 12 males and three juveniles in five slides) are deposited in the collection of the Nematology

Laboratory of Nanjing Agriculture University. ZooBank identifier: 9231E061-2E22-4819-AB76-FEC82FAC21D7.

#### Diagnosis and relationships

*Rotylenchus zhongshanensis* sp. nov. (NAU population) is an amphimictic species characterized by having a conoid rounded lip region with four annuli, lateral field with four lines, stylet 30.1–33.8 µm long, vulva at 48.0–56.5%, rounded tail with thickened cuticle and bearing 20–28 annuli. According to Castillo & Vovlas (2005), *R. zhongshanensis* sp. nov. receives the matrix code as A3, B3, C7, D4, E2, F2, G2, H2, I2, J1, K2.

Based on the number of lip annuli, distance of DGO to stylet base, female vulva position and tail shape, *R. zhongshanensis* sp. nov. is closed to a few *Rotylenchus* species including *Rotylenchus bialaebursus* Van den Berg & Heyns, 1974, *Rotylenchus goodeyi* Loof & Oostenbrink, 1958, *Rotylenchus impar* (Phillips, 1971) Germani et al., 1985, *R. incisicaudatus* (Phillips, 1971) Germani et al., 1985, *Rotylenchus mabelei* Van den Berg & De Waele,

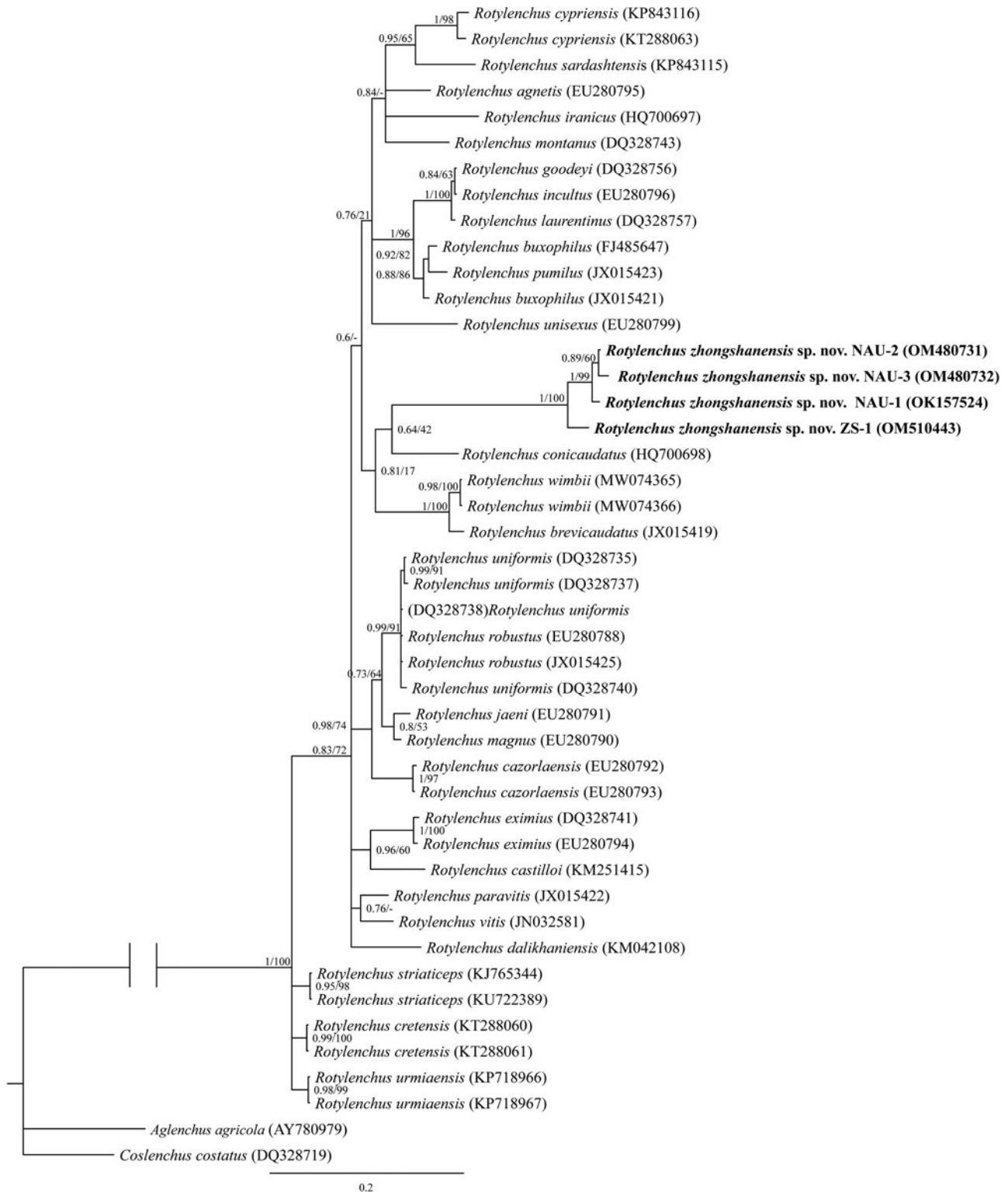


**Fig. 5.** Bayesian 50% majority-rule consensus tree of *Rotylenchus zhongshanensis* sp. nov. and other Hoplolaimidae species inferred from 28S rRNA gene. Dataset aligned with G-INS-i implemented in Multiple Alignment using Fast Fourier Transform. The values at clade node indicate as posterior probability/bootstrap. Newly obtained sequence is indicated in boldface type. The scale bar indicates expected changes per site.

1989 and *Rotylenchus minutus* (Sher, 1963) Germani *et al.*, 1985. However, *R. zhongshanensis* sp. nov. differs from *R. bialaebursus* by the labial region shape (conoid vs. rounded), stylet length (30.1–33.8 vs. 26.1–28.7  $\mu\text{m}$  in female), phasmid position (4–6

annuli posterior to anus vs. 9–12 annuli anterior to anus) and gubernaculum length (5.5–8.0 vs. 11.8–13.2  $\mu\text{m}$ ); from *R. goodeyi* by the female lip region shape (conoid vs. hemispherical), phasmid position (4–6 annuli posterior to anus vs. 1–11 annuli anterior to

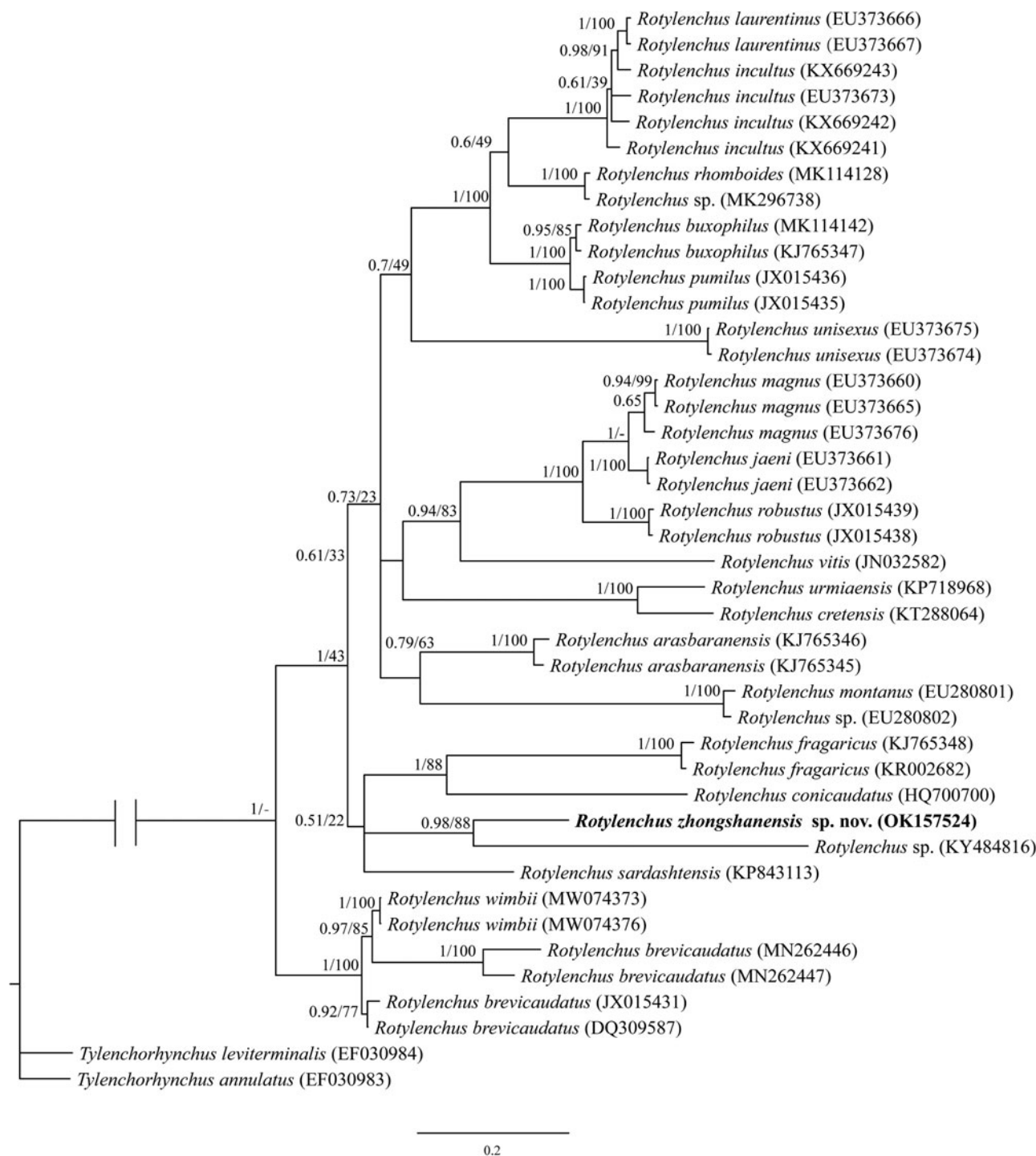


**Fig. 6.** Bayesian 50% majority-rule consensus tree of *Rotylenchus zhongshanensis* sp. nov. and other Hoplolaimidae species inferred from ITS2 region of rRNA genes. Dataset aligned with G-INS-i implemented in Multiple Alignment using Fast Fourier Transform. The values at each clade node indicate as posterior probability/bootstrap. Newly obtained sequence is indicated in bold face type. The scale bar indicates expected changes per site.

anus) and gubernaculum length (5.5–8.0 vs. 13–15  $\mu\text{m}$ ); from *R. mabelei* by lip region shape (conoid, continuous with body contour vs. hemispherical and slightly set off from body), stylet length (30.1–33.8 vs. 27.0–29.5  $\mu\text{m}$ ), body diameter (22.5–34.5 vs. 23–27  $\mu\text{m}$ ), a ratio (22.6–32.2 vs. 35.4–44.2), pharyngeal gland (a very short overlapping not forming a lobe, but abutting in an almost basal bulb-like pharyngeal gland vs. a pharyngeal overlapping lobe), female tail (hemispherical vs. dorsally convex-conoid),

spermatheca (rounded to spherical vs. not developed) and presence of males (vs. absence); from *R. minutus* by the female body length (670.0–927.4 vs. 550–670  $\mu\text{m}$ ), lip region shape (conoid vs. hemispherical), stylet length (30.1–33.8 vs. 21–25  $\mu\text{m}$  in female) and phasmid position (4–6 annuli posterior to anus vs. 3 annuli anterior to anus); from *R. impar* and *R. incisicaudatus* both by the stylet length (30.1–33.8 vs. shorter than 30  $\mu\text{m}$  in female), dorsal pharyngeal gland overlapping (11.2–16.8 vs. 21.0–30.9  $\mu\text{m}$ ), phasmid



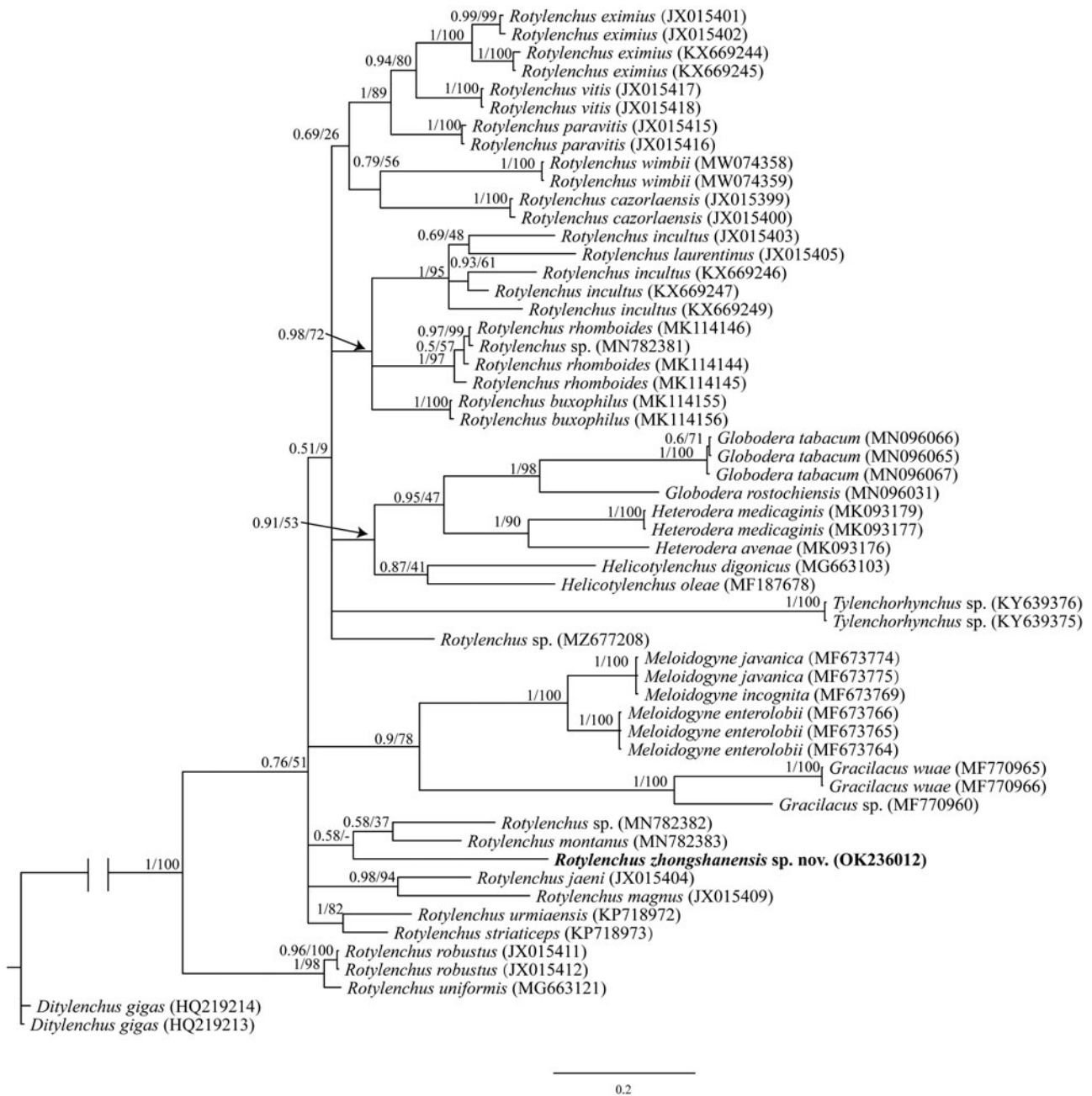


**Fig. 7.** Bayesian 50% majority-rule consensus tree of *Rotylenchus zhongshanensis* sp. nov. and other related species inferred from mitochondrial *COI* gene. Dataset aligned TranslatorX under the invertebrate mitochondrial genetic code. The values at clade node indicate as posterior probability/bootstrap. Newly obtained sequence is indicated in boldface type.

position (4–6 annuli posterior to anus vs. well anterior to anus) and presence of males (vs. absence). Besides, the new species has conoid lip region, while *R. impar* and *R. incisicaudatus* have truncate and rounded labial regions, respectively.

In addition, *R. zhongshanensis* sp. nov. can be separated from the genetically related species by the following characters: different from *Rotylenchus conicaudatus* Atighi *et al.*, 2011 by DGO (3.7–5.0 vs. 6–11  $\mu$ m), pharyngeal glands overlapping (11.2–16.8 vs. 19–33  $\mu$ m), tail shape (hemispherical vs. conoid-rounded) and phasmid position (4–6 annuli posterior to anus vs. 5–12 annuli anterior to anus); different from *Rotylenchus fragaricus* (Maqbool & Shahina, 1986) Atighi *et al.*, 2014 by the lip region

shape (conoid vs. truncate), DGO (3.7–5.0 vs. 7–9  $\mu$ m), pharyngeal glands overlapping (11.2–16.8 vs. 41–58  $\mu$ m), vulva position (48.0–56.5 vs. 59.5–64.0%), presence of males (vs. absence) and phasmid position (4–6 annuli posterior to anus vs. 6–18 annuli anterior to anus); different from *Rotylenchus montanus* Vovlas *et al.*, 2008 by the lip annulation (4 annuli vs. 6 annuli), lip region shape (conoid vs. hemispherical), presence of males (vs. absence), and phasmid position (4–6 annuli posterior to anus vs. 2–9 annuli anterior to anus); and different from *Rotylenchus sardashtensis* Golhasan *et al.*, 2016 (closely related species in ITS phylogeny), by the lip region shape (conoid vs. hemispherical), stylet length (30.1–33.8 vs. 26–30  $\mu$ m), tail shape (hemispherical vs. rounded

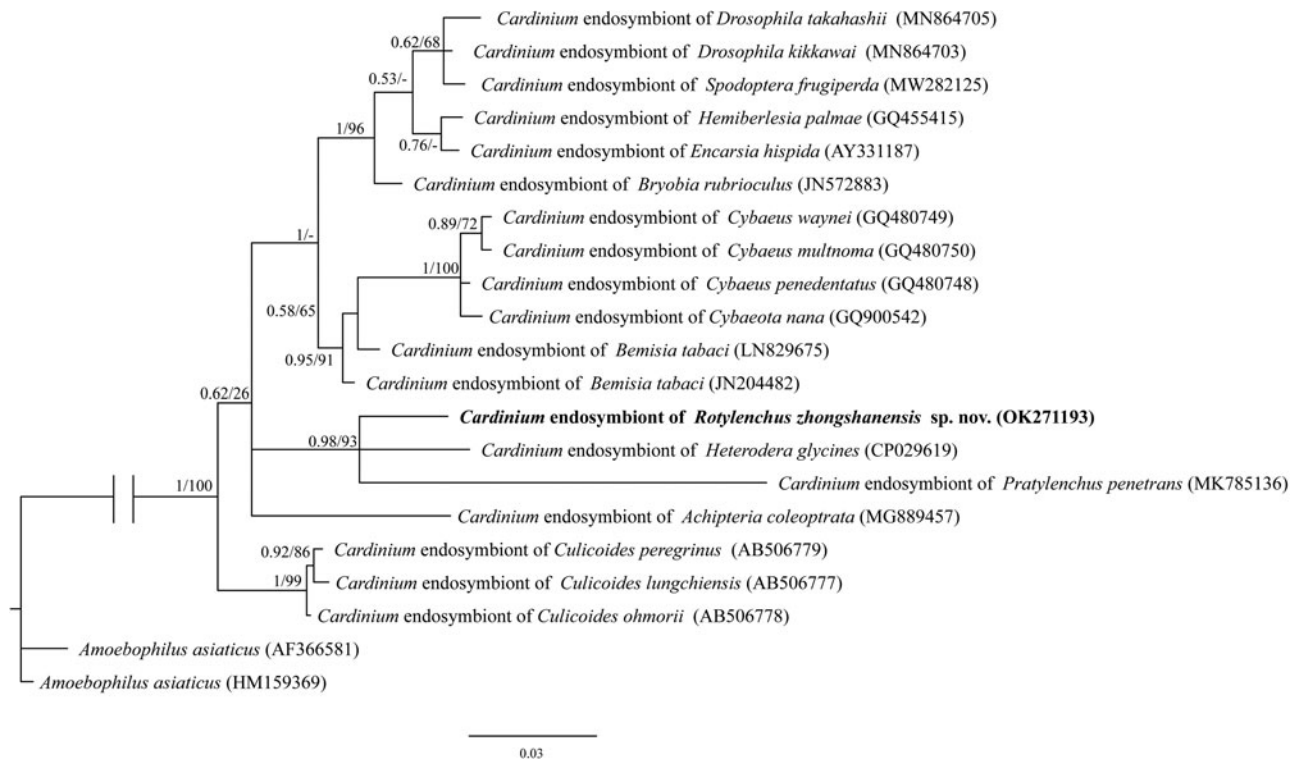


**Fig. 8.** Bayesian 50% majority-rule consensus tree of the new *Cardinium* strain of *Rotylenchus zhongshanensis* sp. nov. and other related *Cardinium* strains inferred from 16S rRNA gene. Dataset aligned with G-INS-i implemented in Multiple Alignment using Fast Fourier Transform. The values at clade node indicate as posterior probability/bootstrap. Newly obtained sequence is indicated in boldface type.

with ventral mucro), V ratio (48.0–56.5 vs. 67.0–77.0%), presence of males (vs. absence), and phasmid position (4–6 annuli posterior to anus vs. 10–23 annuli anterior to anus).

### Molecular characterization and phylogeny

We assembled the full length rRNA gene of *R. zhongshanensis* sp. nov. from the NAU population, and extracted its barcoding regions to infer the corresponding phylogenies. This assembly and extraction yielded 1661 bp 18S sequences (GenBank accession OK256171), 787 bp for D2–D3 domain of 28S and 229 bp for ITS2 (OK157524). The reads mapping to mitochondrial genome reference yielded 1381 bp for partial *COI* gene (OK236012). Additional sequences were obtained through PCR amplification for 18S (OM480710 and OM480711) and 28S (OM480731, OM480732 and OM510443). In comparison with most relevant species in NCBI, the 18S sequence (OK256171) had 95.0% identity with that from *Rotylenchus* sp. (AY284608), differing by 83 nucleotides. For 28S sequence, the NAU population (OK157524) differs from *R. conicaudatus* (HQ700698) by 93 nucleotides (88.0% identity). For ITS sequence, the new species (OK157524) differs from that of *Rotylenchus* sp. (KY484816) by 74 nucleotides (78.0% identity). For *COI* sequence, the new species (OK236012) differs from that of *Rotylenchus* sp. (MN782382) by 63 nucleotides (83.0% identity, 299 out of 362 aligned nucleotides) and from that of *R. montanus* (MN782383) by 68 nucleotides (82.0% identity, 324 out of 392 aligned nucleotides).

Phylogenetic relationships of *R. zhongshanensis* sp. nov. were determined by BI and ML analyses using four markers. In the 18S tree (fig. 4) the new species grouped with an unidentified

*Rotylenchus* sp. (AY284608), forming a well-supported clade (posterior probability (PP) = 1, BS = 100). Intraspecific variation among the 18S gene of the new species are 3–6 nucleotides (99.3–99.7% identity). The 28S phylogeny (fig. 5) grouped the new species with *R. conicaudatus* (HQ700698) in a weakly supported clade (PP = 0.64, BS = 42). Intraspecific variation of 28S gene in NAU population are 6–15 nucleotides, and the representative of NAU population (OK157524) has 30 nucleotides (96.0% identity), which is different from that of ZS population (OM510443). No morphological difference was observed between ZS and NAU populations. In the ITS tree (fig. 6), the new species is sister to an unidentified *Rotylenchus* species (KY484816) (PP = 0.98, BS = 88), but the placement of this clade is unresolved within a less supported clade (PP = 0.51) including *R. conicaudatus*, *R. fragaricus* and *R. sardashtensis*. In the *COI* tree (fig. 7), *R. zhongshanensis* sp. nov. clustered with an unidentified *Rotylenchus* sp. and *R. montanus*, forming a weakly supported clade (PP = 0.58).

### Phylogeny analysis of *Cardinium*

In the process of assembling the *R. zhongshanensis* sp. nov. genome, we found a short sequence (350 bp) belonging to the 16S rRNA gene of a new *Cardinium* endosymbiont strain. The subsequent PCR amplification using two primer pairs resulted in a 16S rRNA fragment of 1285 bp (OK271193). The phylogeny analysis (fig. 8) placed the new *Cardinium* strain of *R. zhongshanensis* sp. nov. within the well-supported clade containing *H. glycines* and *P. penetrans* (PP = 0.98, BS = 93). The 16S rRNA of new *Cardinium* strain differs from the *Cardinium* endosymbiont in *H. glycines* (CP029619) and *P. penetrans* (MK785136) by 51 nucleotides (96.0% identity, 1232 out of 1283 aligned sequences)

and 35 nucleotides (93.0% identity, 457 out of 492 aligned sequences), respectively.

## Discussion

*Rotylenchus zhongshanensis* sp. nov. was morphologically and molecularly characterized in this study. The new species fits the typical generic character of genus *Rotylenchus* in family Hoplolaimidae Filipjev, 1934, including the conoid lip region, very short pharyngeal glands overlapping, phasmids 4–6 annuli posterior to level of anus, and was further characterized by abnormal cuticle thickening in female tail terminus. Unlike other Hoplolaimidae species with distinct pharyngeal glands overlapping, the pharyngeal glands of *R. zhongshanensis* sp. nov. are bulb-shaped with very short overlapping, thus it was preliminarily identified as a member of the controversial genus *Pararotylenchus* Baldwin & Bell, 1981. The separation of *Rotylenchus* and *Pararotylenchus* was based on several characters, perhaps the most important one being that the pharyngeal glands in *Pararotylenchus* are enclosed in a terminal bulb rather than overlapping the intestine (Baldwin & Bell, 1981). However, Brzeski and Choi (1998) rejected the importance of that distinction and proposed the *Pararotylenchus* as a synonym of *Rotylenchus*, but no molecular data on *Pararotylenchus* spp. is currently available for further discussion. In our case, the new species has conoid-rounded lip region, bulb-shaped pharyngeal glands, phasmids near anus and broadly rounded tail, which are similar traits to that of *Pararotylenchus belli* Robbins, 1983. However, after the careful morphological comparison together with the phylogenetic analyses, we confirmed *R. zhongshanensis* sp. nov. as a new taxon in genus *Rotylenchus*. Therefore, the combination of morphological and molecular approaches is warranted to address the limitations of each approach in the identification of *Rotylenchus* species, or plant-parasitic nematodes in general. Nevertheless, additional molecular studies are needed to clarify the validity of the genus *Pararotylenchus* as well as its phylogenetic relationships with *Rotylenchus* spp. for validating or rejecting the proposed synonymy by Brzeski and Choi (1998).

In this study, the partial genome of *R. zhongshanensis* sp. nov. was obtained using the Illumina genomic sequencing technique, and the sequences of rRNA as well as *COI* genes were extracted from the assembled genome. Compared to standard PCR amplification with primer pairs, the used technique is more convenient without amplification, more accurate and less costly. Sometimes, the marker genes of one taxon are difficult to be amplified and the quality of sequences obtained by Sanger sequencing is not high. As the cost of high-throughput sequencing decreases, the genome sequencing may become the common method for acquiring more comprehensive and accurate gene information from nematodes.

A short sequence of a new *Cardinium* strain was also discovered from the *R. zhongshanensis* sp. nov. genome. The bacterial cyto-endosymbionts are critical players in many ecosystems for a number of reasons (Gotoh *et al.*, 2007; Nakamura *et al.*, 2012). They may provide novel biosynthetic capabilities to help supplement nutrients that are limited in their hosts (Brown *et al.*, 2018). The genus *Cardinium* has already recovered from root lesion nematode *P. penetrans* (Denver *et al.*, 2016) and cyst nematodes belonging to genera *Globodera* and *Heterodera* (Shepherd *et al.*, 1973; Endo, 1979; Walsh *et al.*, 1983a, b; Yang *et al.*, 2017). Other endosymbiont bacteria reported from nematodes belong to the genera *Xiphinematocola pachtaicus*,

*Wolbachia* and *Xiphinematobacter* (Haegeman *et al.*, 2009; Palomares-Rius *et al.*, 2014, 2021). During the present study, the endosymbiosis of a *Cardinium* sp. was recovered/proposed for the newly described species of *Rotylenchus* through the Illumina sequencing and subsequent PCR amplification.

## Financial support

This research was supported by the National Natural Science Foundation of China (Grant number 32001876).

## Conflict of interest

None.

## Ethical approval

The conducted research is not either related to human or animals use.

## References

- Abascal F, Zardoya R and Telford MJ (2010) Translator X: Multiple alignment of nucleotide sequences guided by amino acid translations. *Nucleic Acids Research* 38(Web Server issue), W7–W13.
- Aliramaji F, Pourjam E, Álvarez-Ortega S, Pedram M and Atighi MR (2015) *Rotylenchus dalikhaniensis* n. sp. (Nematoda: Hoplolaimidae), a monosexual species recovered from the rhizosphere of *Ruscus hyrcanus* Woronow in Mazandaran province, northern Iran. *Nematology* 17(1), 67–77.
- Atighi MR, Pourjam E, Pedram M, Cantalapiedra-Navarrete C, Palomares-Rius JE and Castillo P (2011) Molecular and morphological characterisations of two new species of *Rotylenchus* (Nematoda: Hoplolaimidae) from Iran. *Nematology* 13(8), 951–964.
- Atighi MR, Pourjam E, Ghaemi R, Pedram M, Liébanas G, Cantalapiedra-Navarrete C, Castillo P and Palomares-Rius JE (2014) Description of *Rotylenchus arasbaranensis* n. sp. from Iran with discussion on the taxonomic status of *Plesiorotylenchus* Vovlas, Castillo and Lamberti, 1993 (Nematoda: Hoplolaimidae). *Nematology* 16(9), 1019–1045.
- Baldwin JG and Bell AH (1981) *Pararotylenchus* n. gen. (Pararotylenchinae n. subfam., Hoplolaimidae) with six new species and two new combinations. *Journal of Nematology* 13(2), 111–128.
- Blaxter ML, De Ley P, Garey JR, *et al.* (1998) A molecular evolutionary framework for the phylum Nematoda. *Nature* 392(6671), 71–75.
- Brown AMV (2018) Endosymbionts of plant-parasitic nematodes. *Annual Review of Phytopathology* 56, 225–242.
- Brown AMV, Wasala SK, Howe DK, Peetz AB, Zasada IA and Denver DR (2018) Comparative genomics of *Wolbachia-Cardinium* dual endosymbiosis in a plant-parasitic nematode. *Frontiers in Microbiology* 9, 2482.
- Brzeski MW, Choi YE (1998) Synonymisation of *Rotylenchus* Filipjev, 1936 and *Pararotylenchus* Baldwin & Bell, 1981 (Nematoda: Hoplolaimidae). *Nematologica* 44(1), 45–48.
- Cantalapiedra-Navarrete C, Liébanas G, Archidona-Yuste A, Palomares-Rius JE and Castillo P (2012) Molecular and morphological characterization of *Rotylenchus vitis* n. sp. (Nematoda: Hoplolaimidae) infecting grapevine in southern Spain. *Nematology* 14(2), 235–247.
- Cantalapiedra-Navarrete C, Navas-Cortés JA, Liébanas G, Vovlas N, Subbotin SA, Palomares-Rius JE and Castillo P (2013) Comparative molecular and morphological characterisations in the nematode genus *Rotylenchus*: *Rotylenchus paravitis* n. sp., an example of cryptic speciation. *Zoologischer Anzeiger – A Journal of Comparative Zoology* 252(2), 246–268.
- Castillo P and Vovlas N (2005) *Bionomics and identification of the genus Rotylenchus* (Nematoda: Hoplolaimidae). *nematology monographs and perspectives* 3. (Series editors: Hunt, D.J. and Perry, R.N.). Leiden, The Netherlands, Brill.
- Cobb NA (1917) A new parasitic nema found infesting cotton and potatoes. *Journal of Agricultural Research* 11, 27–33.

- Coomans A (1962) Morphological observations on *Rotylenchus goodeyi* Loof and Oostenbrink, 1958. *Nematologica* 7(3), 203–215.
- Denver DR, Brown AMV, Howe DK, Peetz AB and Zasada IA (2016) Genome skimming: a rapid approach to gaining diverse biological insights into multicellular pathogens. *PLoS Pathogens* 12(8), e1005713.
- Dierckxsens N, Mardulyn P and Smits G (2017) NOVOPlasty: de novo assembly of organelle genomes from whole genome data. *Nucleic Acids Research* 45(4), e18.
- Endo BY (1979) The ultrastructure and distribution of an intracellular bacterium-like microorganism in tissue of larvae of the soybean cyst nematode. *Heterodera glycines*. *Journal of Ultrastructure Research* 67(1), 1–14.
- Filipjev IN (1934) The classification of free-living nematodes and their relations to parasitic nematodes. *Smithsonian Miscellaneous Collections* 89(6), 1–63.
- Filipjev IN (1936) On the classification of the Tylenchinae. *Proceedings of the Helminthological Society of Washington* 3(2), 80–82.
- Germani G, Baldwin JG, Bell AH and Wu XY (1985) Revision of the genus *Scutellonema* Andrassy 1958 (Nematoda: Tylenchida). *Revue de Nématologie* 8, 289–320.
- Golhasan B, Heydari R, Álvarez-Ortega S, Meckes O, Pedram M and Atighi MR (2016) *Rotylenchus sardashtensis* n. sp., a monosexual species from Iran, with molecular identification and detailed morphological observations on an Iranian population of *Rotylenchus cypriensis* Antoniou, 1980 (Nematoda: Rhabditida: Hoplolaimidae). *Systematic Parasitology* 93(4), 395–411.
- Gotoh T, Noda H and Ito S (2007) *Cardinium* symbionts cause cytoplasmic incompatibility in spider mites. *Heredity* 98(1), 13–20.
- Haegeman A, Vanholme B, Jacob J, Vandekerckhove TT, Claeys M, Borgonie G and Gheysen G (2009) An endosymbiotic bacterium in a plant-parasitic nematode: member of a new *Wolbachia* supergroup. *International Journal for Parasitology* 39(9), 1045–1054.
- Hegedusova E, Brejova B, Tomaska L, Sipiczki M and Nosek J (2014) Mitochondrial genome of the basidiomycetous yeast *Jaminala angkorensis*. *Current Genetics* 60(1), 49–59.
- Hunter MS, Perlman SJ and Kelly SE (2003) A bacterial symbiont in the Bacteroidetes induces cytoplasmic incompatibility in the parasitoid wasp *Encarsia pergandiella*. *Proceedings of the Royal Society B: Biological Sciences* 270(1529), 2185–2190.
- Jones JT, Haegeman A, Danchin EG, et al. (2013) Top 10 plant-parasitic nematodes in molecular plant pathology. *Molecular Plant Pathology* 14(9), 946–961.
- Katoh K and Standley DM (2013) MAFFT multiple sequence alignment software version 7: improvements in performance and usability. *Molecular Biology and Evolution* 30(4), 772–780.
- Li H, Handsaker B, Wysoker A, Fennell T, Ruan J, Homer N, Marth G, Abecasis G and Durbin R (2009) The Sequence Alignment/Map format and SAMtools. *Bioinformatics* 25(16), 2078–2079.
- Loof PAA and Oostenbrink M (1958) Die identität Von *Tylenchus Robustus* De Man [The identity of *Tylenchus robustus* De Man]. *Nematologica* 3(1), 34–43. [In German.]
- Maqbool MA and Shahina F (1986) Four new species of the family Hoplolaimidae: (Nematoda) with notes on *Rotylenchus cypriensis* Antoniou from Pakistan. *Nematologia Mediterranea* 14(1), 117–128.
- Miller MA, Pfeiffer W and Schwartz T (2010) Creating the CIPRES science gateway for inference of large phylogenetic trees. In *Proceedings of the Gateway Computing Environments Workshop (GCE) LA*, New Orleans, LA, USA, 14 November 2010. Piscataway, NJ, Institute of Electrical and Electronics Engineers, pp. 1–8.
- Nadler S, Felix MA, Frisse L, Sternberg PW, De Ley P and Thomas WK (1999) Molecular and morphological characterisation of two reproductively isolated species with mirror-image anatomy (Nematoda: Cephalobidae). *Nematology* 1, 591–612.
- Nakamura Y, Yukuhiro F, Matsumura M and Noda H (2012) Cytoplasmic incompatibility involving *Cardinium* and *Wolbachia* in the white-backed planthopper *Sogatella furcifera* (Hemiptera: Delphacidae). *Applied Entomology and Zoology* 47(3), 273–283.
- Nguyen HT, Trinh QP, Couvreur M, Singh PR, Decraemer W and Bert W (2019) Description of *Rotylenchus rhomboides* n. sp. and a Belgian population of *Rotylenchus buxophilus* (Tylenchomorpha: Hoplolaimidae). *Journal of Nematology* 51, e2019–e2023.
- Noel GR and Atibalentja N (2006) ‘*Candidatus* Paenicardinium endonii’, an endosymbiont of the plant-parasitic nematode *Heterodera glycines* (Nematoda: Tylenchida), affiliated to the phylum Bacteroidetes. *International Journal of Systematic and Evolutionary Microbiology* 56(7), 1697–1702.
- Noruzi E, Asghari R, Atighi MR, Eskandari A, Cantalapedra-Navarrete C, Archidona-Yuste A, Liébanas G, Castillo P and Palomares-Rius JE (2015) Description of *Rotylenchus urmiaensis* n. sp. (Nematoda: Hoplolaimidae) from North-western Iran with a molecular phylogeny of the genus. *Nematology* 17(5), 607–619.
- Palomares-Rius JE, Cantalapedra-Navarrete C and Castillo P (2014) Cryptic species in plant-parasitic nematodes. *Nematology* 16(10), 1105–1118.
- Palomares-Rius JE, Archidona-Yuste A, Cantalapedra-Navarrete C, Prieto P and Castillo P (2016) Molecular diversity of bacterial endosymbionts associated with dagger nematodes of the genus *Xiphinema* (Nematoda: Longidoridae) reveals a high degree of phylogenetic congruence with their host. *Molecular Ecology* 25(24), 6225–6247.
- Palomares-Rius JE, Gutiérrez-Gutiérrez C, Mota M, et al. (2021) ‘*Candidatus* Xiphinematocola pachtaicus’ gen. nov., sp. nov., an endosymbiotic bacterium associated with nematode species of the genus *Xiphinema* (Nematoda, Longidoridae). *International Journal of Systematic and Evolutionary Microbiology* 71(7), 004888.
- Phillips SP (1971) Studies of plant and soil nematodes. 16. Eight new species of spiral nematodes (Nematoda: Tylenchoidea) from Queensland. *Queensland Journal of Agricultural and Animal Sciences* 28(4), 227–242.
- Robbins RT (1983) Description of *Pararotylenchus belli* n. sp. (Nematoda: Hoplolaimidae). *Journal of Nematology* 15(3), 353–356.
- Ronquist F, Teslenko M, van der Mark P, et al. (2012) MrBayes 3.2: efficient Bayesian phylogenetic inference and model choice across a large model space. *Systematic Biology* 61(3), 539–542.
- Sedlazeck FJ, Rescheneder P and von Haeseler A (2013) NextGenMap: fast and accurate read mapping in highly polymorphic genomes. *Bioinformatics* 29(21), 2790–2791.
- Shepherd AM, Clark SA and Kempton A (1973) An intracellular microorganism associated with tissues of *Heterodera* spp. *Nematologica* 19(1), 31–34.
- Sher SA (1963) Revision of the Hoplolaiminae (Nematoda) III. *Scutellonema* Andrassy, 1958. *Nematologica* 9(3), 421–443.
- Showmaker KC, Walden KKO, Fields CJ, Lambert KN and Hudson ME (2018) Genome sequence of the soybean cyst nematode (*Heterodera glycines*) endosymbiont ‘*Candidatus* *Cardinium hertigii*’ strain cHgTN10. *Genome Announcements* 6(26), e00624–18.
- Singh PR, Nyiragatare A, Janssen T, Couvreur M, Decraemer W and Bert W (2018) Morphological and molecular characterisation of *Pratylenchus rwandae* n. sp. (tylenchida: Pratylenchidae) associated with maize in Rwanda. *Nematology* 20(8), 781–794.
- Singh PR, van de Vossenberg B, Rybarczyk-Mydlowska K, Kowalewska-Groszkowska M, Bert W and Karssen G (2021) An integrated approach for synonymization of *Rotylenchus rhomboides* with *R. goodeyi* (Nematoda: Hoplolaimidae) reveals high intraspecific mitogenomic variation. *Phytopathology* 112(5), 1152–1164.
- Sohlenius B and Sandor A (1987) Vertical distribution of nematodes in arable soil under grass (*Festuca pratensis*) and barley (*Hordeum distichum*). *Biology and Fertility of Soils* 3(1–2), 19–25.
- Stamatakis A, Hoover P and Rougemont J (2008) A rapid bootstrap algorithm for the RAxML web servers. *Systematic Biology* 57(5), 758–771.
- Talezari A, Pourjam E, Kheiri A, Liebanas G, Aliramaji F, Pedram M, Rezaee S and Atighi MR (2015) *Rotylenchus castilloi* n. sp. (Nematoda: Hoplolaimidae), a new species with long stylet from northern Iran. *Zootaxa* 3931(1), 88–100.
- Tzortzakakis EA, Archidona-Yuste A, Liébanas G, Birmpilis IG, Cantalapedra-Navarrete C, Navas-Cortés JA, Castillo P and Palomares-Rius JE (2016) *Rotylenchus cretensis* n. sp. and *R. cypriensis* Antoniou 1980 (Nematoda: Hoplolaimidae) recovered from the rhizosphere of olive at Crete (Greece) with a molecular phylogeny of the genus. *European Journal of Plant Pathology* 144(1), 167–184.
- Vandekerckhove TT, Willems A, Gillis M and Coomans A (2000) Occurrence of novel verrucocomicrobial species, endosymbiotic and

- associated with parthenogenesis in *Xiphinema americanum*-group species (Nematoda, Longidoridae). *International Journal of Systematic and Evolutionary Microbiology* **50**(6), 2197–2205.
- Van den Berg E and Heyns J** (1974) South African Hoplolaiminae. 3. The genus *Rotylenchus* Filipjev, 1936. *Phytophylactica* **6**, 165–184.
- Vovlas N, Subbotin SA, Troccoli A, Liébanas G and Castillo P** (2008) Molecular phylogeny of the genus *Rotylenchus* (Nematoda, Tylenchida) and description of a new species. *Zoologica Scripta* **37**(5), 521–537
- Walsh JA, Lee DL and Shepherd AM** (1983a) The distribution and effect of intracellular rickettsia-like microorganisms infecting adult males of the potato cyst-nematode *Globodera rostochiensis*. *Nematologica* **29**(2), 227–239.
- Walsh JA, Shepherd AM and Lee DL** (1983b) The distribution and effect of intracellular rickettsia-like microorganisms infecting second-stage juveniles of the potato cyst-nematode *Globodera rostochiensis*. *Journal of Zoology* **199** (3), 395–419.
- Weeks AR, Velten R and Stouthamer R** (2003) Prevalence of a new sex ratio distorting endosymbiotic bacterium among arthropods. *Proceedings of the Royal Society B: Biological Sciences* **270**(1526), 1857–1865.
- White JA, Kelly SE, Cockburn SN, Perlman SJ and Hunter MS** (2011) Endosymbiont costs and benefits in a parasitoid infected with both *Wolbachia* and *Cardinium*. *Heredity* **106**(4), 585–591.
- Whitehead AG and Hemming JR** (1965) A comparison of some quantitative methods of extracting small vermiform nematodes from soil. *Annals of Applied Biology* **55**(1), 25–38.
- Yang D, Chen C, Liu Q and Jian H** (2017) Comparative analysis of pre- and post-parasitic transcriptomes and mining pioneer effectors of *Heterodera avenae*. *Cell and Bioscience* **7**, 11.
- Zchori-Fein E, Perlman SJ, Kelly SE, Katzir N and Hunter MS** (2004) Characterization of a 'Bacteroidetes' symbiont in *Encarsia* wasps (Hymenoptera: Aphelinidae): proposal of 'Candidatus *Cardinium hertigii*'. *International Journal of Systematic and Evolutionary Microbiology* **54**(3), 961–968.